

New perspectives in bio-analytical techniques for preclinical characterization of a drug candidate: UPLC-MS/MS in *in vitro* metabolism and pharmacokinetic studies

Samuele Pedraglio*, Marco Giulio Rozio, Paola Misiano,
Veronica Reali, Giulio Dondio, Chiara Bigono

NiKem Research S.r.l., V. Zambelletti 25, 20021 Baranzate, Milano, Italy

Received 3 July 2006; received in revised form 11 December 2006; accepted 12 December 2006

Available online 17 December 2006

Abstract

Lead optimization requires rapid bio-analytical turnover for the generation of early absorption, distribution, metabolism, excretion (ADME) and pharmacokinetics (PK) data maintaining a high quality level. Therefore, one of the major challenges in the bio-analytical field is to achieve faster and more sensitive quantification protocols.

In the present communication, a comparison between HPLC and ultra performance liquid chromatography (UPLC) performances in terms of sensitivity and resolution is shown using a pharmacokinetic study and a metabolism study as models. The studies highlight the features of the new technology and the resulting impact in the PK throughput and in the characterization of isomeric metabolites using UPLC/MS/MS technique.

© 2006 Elsevier B.V. All rights reserved.

Keywords: UPLC; HPLC; MS/MS; ADME; Pharmacokinetic; Hepatocytes; Dog; Verapamil; Metabolite; Bioanalytical

1. Introduction

In the recent years, a shift in the strategy of the drug discovery process has occurred underlining the need for very early optimization of the pharmacokinetic characteristics of the novel chemical entities (NCEs). Effective acceleration of the new paradigm for lead optimization requires rapid sample turnover for the generation of early ADME and PK data maintaining a high quality level [1].

Therefore, one challenge in the bio-analytical field is to achieve faster and more sensitive quantification protocols, taking into account matrix interference and method robustness but maintaining at the same time a high throughput.

A second challenge is metabolite identification in matrices such as microsomes and hepatocytes which are often used as tools for preliminary screening. Increased resolution as well as the speed of the method are key issues in the separation of isomeric metabolites.

UPLC-MS/MS was introduced into the analytical equipment market as a new tool showing several advantages including (i) increase in resolution and sensitivity (ii) decrease in analysis time [2,3]. UPLC columns are certified to work under very high pressure, up to 14,000 psi; this feature, coupled with the very small particle size of the stationary phase and the low instrument dead volume, should allow the development of fast and efficient separation methods.

In this work, a comparison between a previously validated HPLC-MS/MS method on a proprietary pre-clinical antitumor candidate (NiK-12192, Fig. 1, inset A) and the new UPLC-MS/MS is presented focusing in particular on the impact of the new technology on the sensitivity and speed of the method.

Comparison of resolution was instead performed during the *in vitro* identification of verapamil metabolites after incubation with dog hepatocytes.

Biotransformations of verapamil are well documented with rat hepatocytes [4] while only few references are known on dog hepatocytes [5].

A comparison of the intrinsic clearance and biotransformation profiles using cryopreserved and fresh dog hepatocytes was

* Corresponding author. Tel.: +39 02 356947548; fax: +39 02 356947606.
E-mail address: samuele.pedraglio@nikemresearch.com (S. Pedraglio).
URL: www.nikemresearch.com.

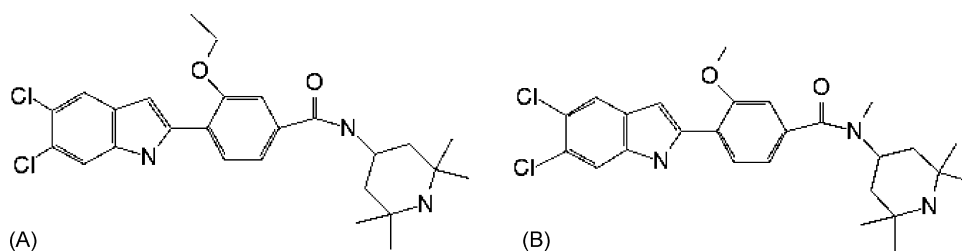


Fig. 1. (A) Structure of NiK-12192. (B) Structure of NiK-12193.

performed and preliminary results suggest significant differences between the two matrices.

2. Experimental

2.1. Reagents and materials

Cryopreserved dog hepatocytes and hepatocyte isolation kits were purchased from XenoTech LLC. Fresh dog hepatocytes were purchased from Biopredic (Rennes, France). Verapamil, formic acid, acetonitrile and ammonia were purchased from Sigma–Aldrich. NiK-12192 and NiK-12193 (Fig. 1, inset B) were synthesized in NiKem Research. Heparin was purchased from Marvecs Services (Agrate Brianza, Italy). HPLC grade water (>18 M Ω) was obtained from a Milli-Q Academic water purification system (Millipore Corporation, Millford, USA). MultiScreen DW Solvinert Filter Plate MDRP-NP4 0.45 μ m PTFE membranes were purchased from Millipore Corporation (Millford, USA). Drug-free heparinized mouse plasma were purchased from Charles-River Italia (Calco, Italy).

2.2. Equipment

Analyses were acquired on a Waters UPLC system with a Sample Organizer coupled with a triple quadrupole Quattro Premiere/XE mass spectrometer (Waters, Milford, USA). The previously validated method was acquired on the same mass spectrometer coupled with a 1525 μ HPLC pump (Waters) and 2777 autosampler (Waters).

2.3. Pharmacokinetic treatment

Thirty-nine nude female HT29/Mit xenograft mice were treated with NiK-12192. The treatments were conducted using two groups of animals. Group 1 ($n = 21$) received an intravenous (rapid bolus) administration of NiK-12192 at 3 mg/kg. Group 2 ($n = 18$) received an oral (gavage) dose of 6 mg/kg. Animal treatments were performed at Istituto Nazionale Tumori (Milano, Italy).

NiK-12192 was prepared in ethanol–cremophor–saline (5:5:90, v/v/v) both for i.v. and for oral administration. Plasma samples were treated with heparin.

2.4. Plasma samples preparation

For the calibration curves and QC, NiK-12192 Stock Solution (10 μ l) at 10 concentrations (1–5000 ng/ml), 10 μ l of the internal

standard (I.S.) at a fixed concentration (500 ng/ml of NiK-12192, a congener of NiK-12192, in acetonitrile) and 15 μ l ammonia (3%, v/v) were added to 90 μ l of drug-free mouse plasma. For the PK sample analysis, plasma samples (100 μ l) were spiked with 10 μ l of I.S. (500 ng/ml) and with 15 μ l ammonia (3%, v/v); proteins were crashed by adding 300 μ l acetonitrile followed by 2 min vortex mixing. Samples were transferred to Solvinert filter plate and mixed for 10 min. The plate was filtered under vacuum; 5 μ l aliquots of the collected samples were injected into the LC/MS/MS system.

2.5. Assay validation

Three standard curves with 10 concentrations of NiK-12192 were prepared and analyzed concurrently with each QC and unknown sample set.

Standard calibration graphs were constructed by linear least-squares regression analysis on the analyte/I.S. area ratio plotted against sample concentration. The lowest calibration point correspond to the limit of quantitation (LOQ), i.e. the lowest concentration that could be measured with acceptable accuracy and precision (>80%). In each study, LOQ concentrations were accepted when the ratio between peak area of the standard plasma samples and that of the blank sample was more than 10.

The upper limit of quantitation (ULOQ) was arbitrarily defined as 500 ng/ml, using 90 μ l of mouse plasma.

Intra-assay precision values were determined in triplicates at different concentrations between LLOQ and 50 ng/ml final concentration in mouse plasma.

Inter-assay precision was evaluated across different concentrations on three different days and the mean concentrations and coefficients of variation were calculated.

The recovery of NiK-12192 was estimated by comparing the peak area of the extracted NiK-12192 to that of the analyte diluted stock solutions at all concentrations.

2.6. LC chromatographic and mass spectrometric conditions

NiK-12192 and I.S. were detected during a gradient elution from phase A water–acetonitrile–formic acid (95/5/0.1, v/v/v) to phase B water–acetonitrile–formic acid (5/95/0.1, v/v/v). Details of the gradients, according to the column used, are reported in Tables 1 and 2. The run time was 3.5 min with the Luna and the XBridge columns while it was 1.5 min with BEH column. The LC eluate was introduced into the API source directly without splitting.

Table 1
Gradient program used with either Luna or XBridge column for PK analysis of NiK-12192

Flow (ml/min)	Time (min)	%A	%B
0.25	0.0	95	5
	0.5	95	5
	0.7	25	75
	1.7	25	75
	1.8	0	100
	2.2	0	100
	2.2	95	5
	3.5	95	5

The mass spectrometer was operated using electrospray interface (ESI) with a capillary voltage of 3.5 kV, cone voltage 30 V, ion source and desolvation gas 100 and 900 l/h, source and desolvation temperature 150 and 500 °C. The positive multiple-reaction-monitoring (MRM) analysis was performed using argon as collision gas with a cell pressure setted at 3.3×10^{-3} mbar.

The following MRM transitions were monitored: m/z 487.8/331.8 for NiK-12192 and m/z 488.0/317.8 for I.S.; for both the transitions the collision energy was settled at 28 eV. During acquisitions, a dwell time of 200 ms with an inter-scan and inter-channel delays of 50 ms was used.

The analyses were performed using either an Acquity BEH C18 column 50 mm \times 2.1 mm \times 1.7 μ m or a Phenomenex Luna C18 5.0 \times 2.1 mm \times 5 μ m (Chemtek, Bologna, Italy) or a Waters XBridge C18 50 mm \times 2.1 mm \times 3.5 μ m.

2.7. Hepatocytes incubation

Cryopreserved dog hepatocytes were thawed using XenoTech's hepatocytes isolation kit and re-suspended in Krebs–Henseleit Medium (KHB, pH 7.4); hepatocytes (final concentration 0.5e6 cells/ml) were incubated with compounds (final concentrations 2.5 μ M for clearance) for 120 min at 37 °C in an incubator (5% CO₂). Fresh dog hepatocytes were reactivated following the producer's protocol and then incubated as for cryopreserved ones.

Samples, taken at 0, 15, 30, 60 and 90 min, were added to acetonitrile, centrifuged and the supernatant was analyzed by LC/MS/MS.

2.8. Clearances and metabolites LC/MS/MS detection

Parent compound and metabolites were simultaneously detected during a gradient elution from 98% phase A

Table 2
Gradient program used Acquity BEH column for PK analysis of NiK-12192

Flow (ml/min)	Time (min)	%A	%B
0.5	0.0	60	40
	0.2	60	40
	0.21	0	100
	1.0	0	100
	1.1	60	40
	1.5	60	40

water–acetonitrile–formic acid (95/5/0.1, v/v/v) to 100% phase B water–acetonitrile–formic acid (5/95/0.1, v/v/v) using the waters system UPLC/Quattro Premiere XE.

The samples were analyzed on an Acquity™ BEH C18 column 50 mm \times 2.1 mm \times 1.7 μ m while metabolic profiles were acquired using an Acquity™ BEH C18 100 mm \times 2.1 mm \times 1.7 μ m. Additional run for comparative purpose were performed with a XBridge C18 100 mm \times 2.1 mm \times 3.5 μ m.

Clearances were calculated by the parent depletion method acquiring the verapamil parent transition m/z 455.2/164.95.

Metabolic transformations were detected by MS full scan followed by MS/MS acquisitions and analyzed by Metabolynx™ software.

3. Results and discussion

3.1. Method development and pharmacokinetic analysis

The aim of this work was the re-validation of the method of analysis of NiK-12192 using the UPLC and the comparison of these new results with those previously obtained on an HPLC system.

In order to explore the performance of the BEH column, the lowest calibration samples were also injected onto the equivalent XBridge column having the same stationary phase as the BEH column but with a larger particle size: 3.5 μ m versus 1.7 μ m.

The extraction method based on the use of Millipore Filter Plate was simple and effective in removing interference from endogenous components. Unfortunately preparation of the samples directly in the extraction plate without pre-mixing in Eppendorfs was about 60%; therefore, samples were pre-mixed in Eppendorfs and then filtered on the plate. In this way, mean overall recoveries averaged 102 ± 7 and $95 \pm 5\%$ at each concentration of NiK-12192 considering either analyte area or analyte/I.S. area ratio, respectively (Table 3).

Samples, prepared as previously described, were analyzed using gradient programs as reported in Tables 1 and 2.

The BEH column showed a higher sensitivity than the XBridge and the Luna columns. In fact, the lower concentra-

Table 3
Mean recoveries from spiked plasma

Tissue (ml)	Conc. (ng/ml)	Recovery area (% \pm S.D.) ^a	Recovery ratio (% \pm S.D.) ^b
Mouse plasma (0.1) (n = 3)	0.1	102.8 \pm 6.6	97.6 \pm 14.9
	0.25	115.6 \pm 3.1	105.4 \pm 3.5
	0.5	98.3 \pm 5.0	94.0 \pm 5.5
	1	87.0 \pm 9.7	95.7 \pm 2.5
	2.5	98.9 \pm 7.1	79.3 \pm 4.1
	5	109.6 \pm 2.0	87.7 \pm 6.8
	10	96.3 \pm 6.6	101.6 \pm 5.3
	25	102.3 \pm 15.0	99.9 \pm 4.5
	50	104.1 \pm 4.0	95.2 \pm 5.5
	100	110.5 \pm 15.0	96.4 \pm 5.0

^a Based on analyte area.

^b Based on ratio between analyte area and I.S. area.

Table 4
LOQ study in UPLC/HPLC conditions

Column	R.T.	Blank area ^a	Mean LOQ area ^a	C.V.%
BEH (0.1 ng/ml)	0.81	6	81.33	3.95
X Bridge (0.5 ng/ml)	1.81	26	254.67	3.34
Luna (1 ng/ml)	1.58	25	261.33	6.36

^a Each result is the mean of three analysis.

tions determined with acceptable accuracy and precision were 0.1, 0.5 and 1 ng/ml, respectively. Both analyte and I.S. peaks were sharper.

In Table 4, a comparison of the conditions and performances for the two techniques is shown: the RT obtained with UPLC column was halved with respect to the HPLC (0.81 and 1.58 min, respectively), peak width was reduced from about 0.08 min to 0.03 min with the acquity column, resulting in an increased Signal to Noise ratio (Figs. 2–4). The reduction of the total run time using UPLC is very significant if considering the overall number of samples in the kinetic study. Shortening of the time of analysis (1.5 min versus 3.5 min) is a consequence of the decrease in particle size and also of the faster reconditioning of the BEH column.

Among the two HPLC columns, better results in terms of LOQ concentration and peak shape were obtained using the XBridge column (Fig. 3) than the Luna column (Fig. 2), even though under the same gradient conditions, R.T. was a little bit shorter for the Luna column than the other due to the larger particle size.

Table 5
Linearity and precision of calibration curves in plasma

Calibration	Corr. coefficient	Slope
$y = 0.105551x + 0.0289918$	0.9998	0.1056
$y = 0.104407x + 0.0327729$	0.9995	0.1044
$y = 0.0950653x + 0.0509373$	0.9996	0.0951
Mean	0.9996	0.1017
S.D.	0.0002	0.0058
C.V.%	0.0153	5.6575

For these concentrations, reported in Table 4, of NiK-12192, C.V. for precision and reproducibility of the assay were both below 6.3%.

Table 5 shows that the relationship between NiK-12192/I.S. area ratios and the amount of compound added to plasma were always linear, with a mean correlation coefficient exceeding 0.9996. The slopes of the three curves prepared on three different days had a mean coefficient of variation (C.V.) of 5.6%.

Reproducibility of the method was evaluated analysing three replicates of QC samples containing the compound at nominal concentrations of 0.1, 0.25, 0.5, 1, 2.5, 10, 50 ng/ml on three different days. The intra- and inter-day precision, expressed as C.V., and accuracy, expressed as relative error (R.E.) are reported in Table 6. The method was found to be precise within acceptable limits, with C.V. <12% and R.E. ranging from –3 to 13%, in the range of tested concentrations.

The influence of the lower LOQ (0.1 pg/ml versus 0.5 ng/ml) is clearly visible in Fig. 5 where the distribution of NiK-12192

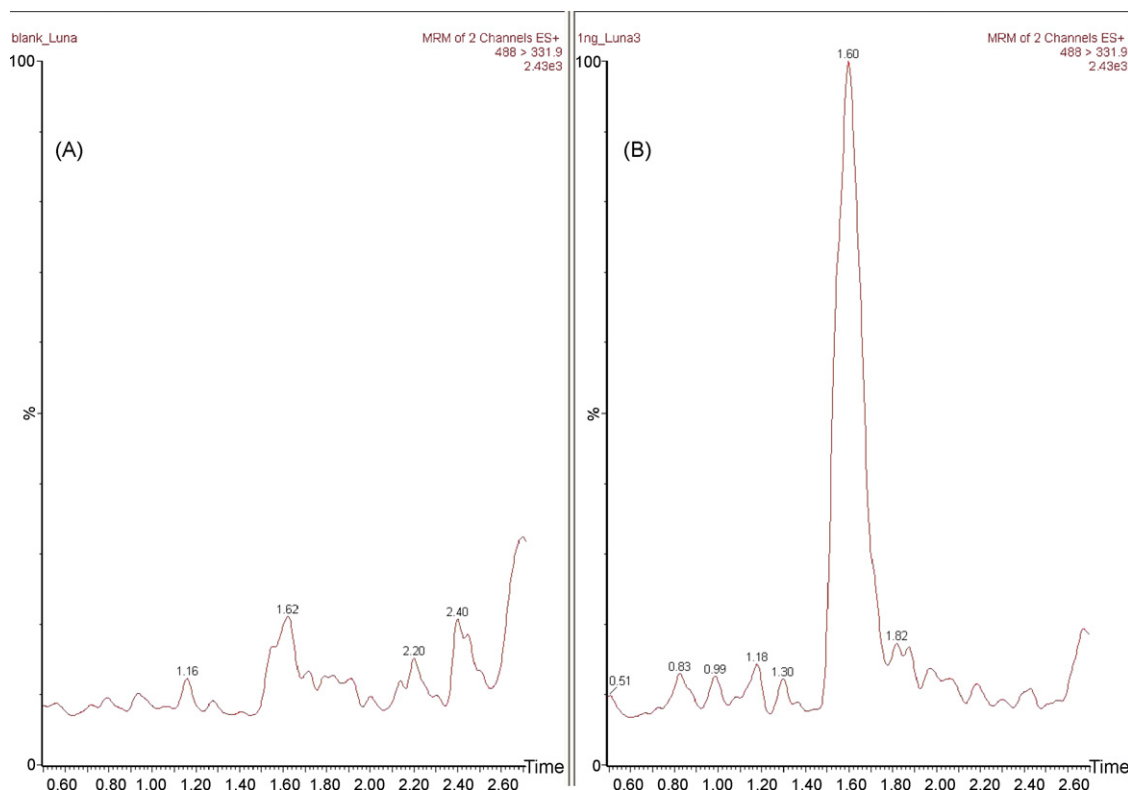


Fig. 2. (A) Chromatogram of blank plasma sample. (B) Chromatogram of spiked plasma sample at the LOQ concentration. Both the chromatograms were obtained under the optimized conditions using Luna C18 50 mm × 2.1 mm × 5 μm column.

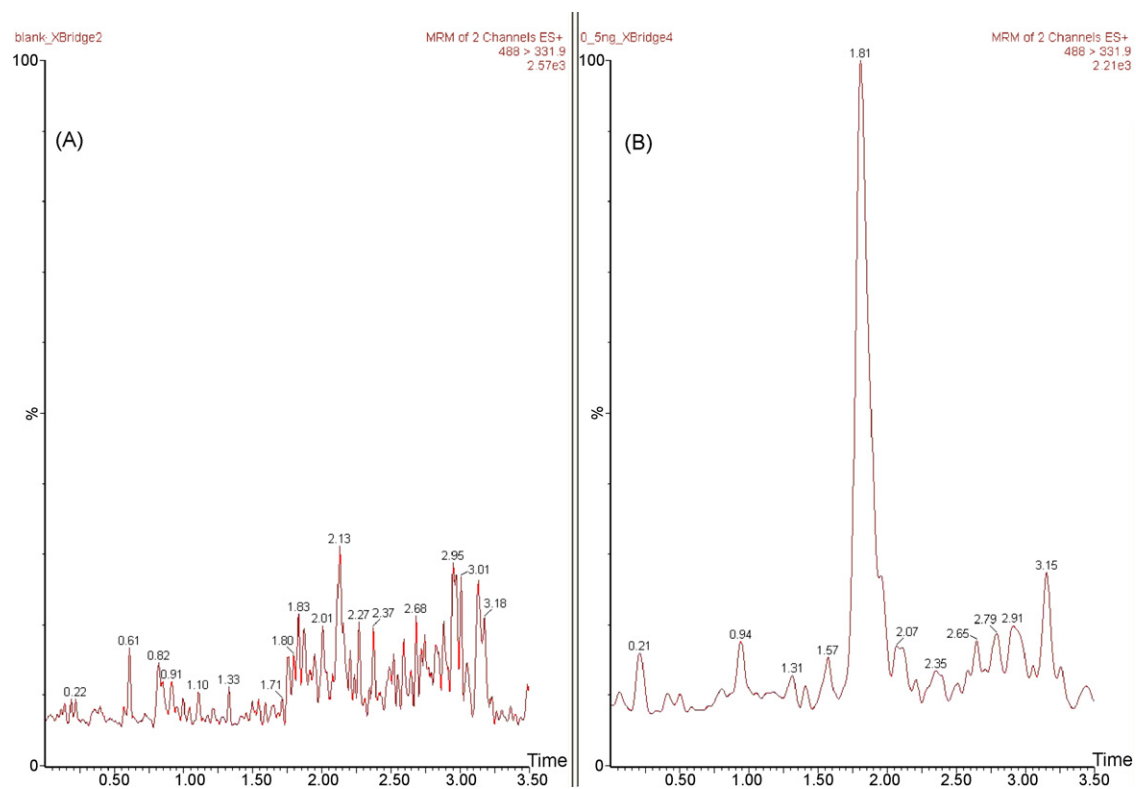


Fig. 3. (A) Chromatogram of blank plasma sample. (B) Chromatogram of spiked plasma sample at the LOQ concentration. Both the chromatograms were obtained under the optimized conditions using XBridge C18 $50 \times 2.1 \text{ mm} \times 3.5 \mu\text{m}$ column.

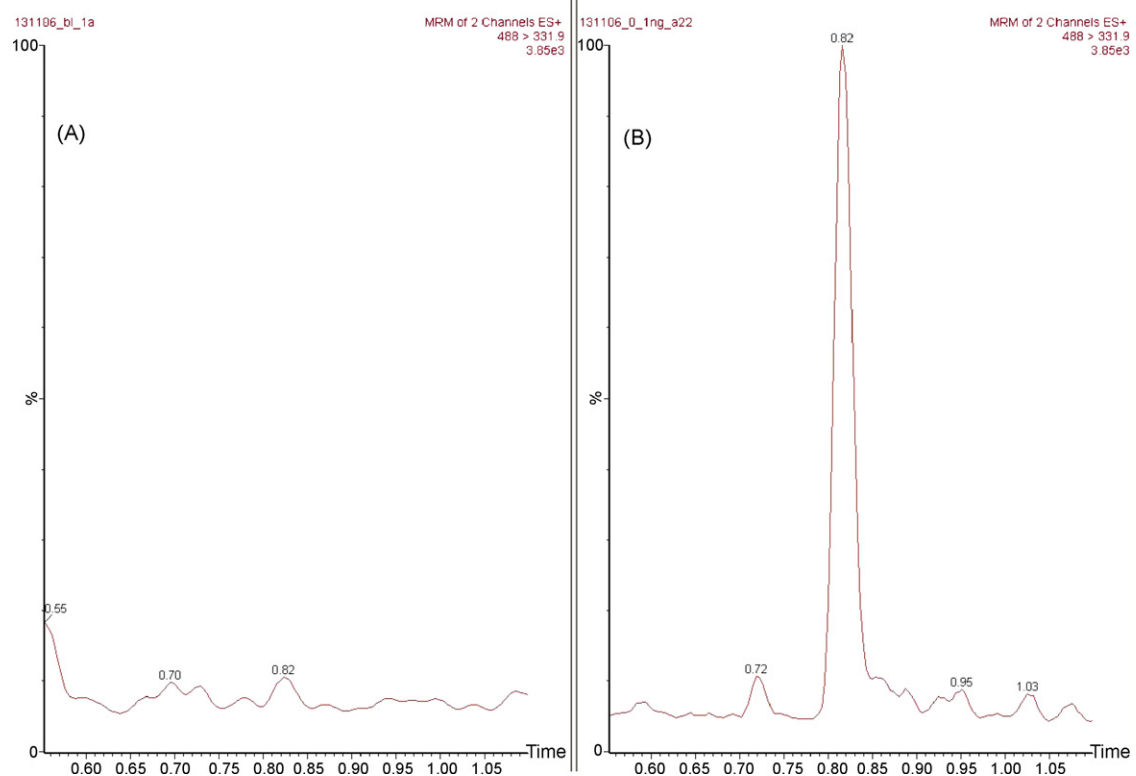


Fig. 4. (A) Chromatogram of blank plasma sample. (B) Chromatogram of spiked plasma sample at the LOQ concentration. Both the chromatograms were obtained under the optimized conditions using Acquity BEH C18 $50 \text{ mm} \times 2.1 \text{ mm} \times 1.7 \mu\text{m}$ column.

Table 6
Summary of intra- and inter-assay precision and accuracy data in Q.C. samples

	Added (ng/ml)	Mean (ng/ml)	R.E. ^a	C.V.%
Within-day (n=3)	0.1	0.100	0.333	0.575
	0.25	0.280	12.000	7.143
	0.5	0.500	0.067	0.115
	1	0.967	-3.333	11.945
	2.5	2.733	9.333	2.112
	10	10.733	7.333	3.272
	50	52.333	4.667	7.234
Day to day (n=3)	0.1	0.100	0.333	0.498
	0.25	0.283	13.022	8.171
	0.5	0.500	0.044	0.088
	1	0.989	-1.111	7.905
	2.5	2.656	6.222	4.655
	10	10.778	7.778	3.034
	50	49.967	-0.067	11.250

^a (Calculated–nominal/nominal) × 100.

in plasma is reported both under HPLC and UPLC conditions. LLOQ with the HPLC column did not allow quantitation at 24 h, affecting the profile of the elimination phase. Analysis by UPLC allowed the quantitation of the 24 h samples indicating a different elimination phase thus affecting significantly the evaluation of the pharmacokinetic parameters and oral bioavailability.

3.2. Clearance and biotransformation studies in fresh and cryopreserved dog hepatocytes

As described above for the PK data, we can expect also similar performance for the determination of in vitro clearance obtaining a significant reduction in the time of analysis.

The clearance of verapamil was studied in fresh and cryopreserved dog hepatocytes and are expressed as $\mu\text{l}/10\text{e}6$ cells; the experimental values are reported in Table 7.

Clearance activity with fresh hepatocytes was much higher than with the cryopreserved contrary to Griffin and Houston [6] who reported differences within two folds. Differences are

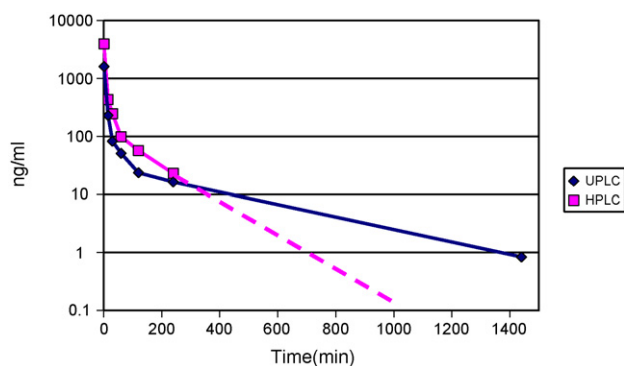


Fig. 5. Plasma distribution of NiK-12192 after I.V. treatment. Dashed lines is an extrapolation of the plasma sample concentration. The real value has not been detected due to the higher value of the LOQ respect to UPLC values. The elimination phase determined in this condition is clearly wrong.

Table 7

Clearance values for verapamil in fresh and cryopreserved hepatocytes, results expressed as mean \pm S.D. (n=3)

Cryopreserved cli ($\mu\text{l}/\text{min}/10\text{e}6$ cells)	Fresh Cli ($\mu\text{l}/\text{min}/10\text{e}6$ cells)
13.0 ± 4.0	92.8 ± 5.8

reflected also in the metabolic profiles (Fig. 6 for fresh, inset A and for cryopreserved, inset B, respectively).

Verapamil is metabolised via *N*-dealkylation, *N*-demethylation and *O*-demethylation, phase II metabolites (glucuronides) were also present.

The dog chromatogram with cryopreserved hepatocytes showed one major peak with $\text{RT}=8.17$ min and mass of $m/z=441$; its fragmentation pattern suggested nor-verapamil as a predominant metabolite. The second most intense peak with $\text{RT}=7.0$ min and mass of $m/z=291$ was assigned to phenyl-isopropyl-valeronitrile whereas all the other peaks displayed a relative low intensity compared to the first two. The other peaks were assigned either to *O*-glucuronated nor-verapamil ($m/z=603$) or to various hydroxylated forms ($m/z=471$). In Table 8 are reported the assigned structures and relative fragments of the metabolites. Four different glucuronides were identified for the demethyl-norverapamil ($m/z=603$) and four other peaks with $m/z=617$ were attributed to demethyl-verapamil glucuronides. For both glucuronides and hydroxylated metabolites it was possible to distinguish which part of the molecule was subjected to metabolic transformation by analyzing the fragmentation pattern: a signal at $m/z=151$ refers to a desmethyl-phenyl-ethyl moiety which corresponds to the fragment $m/z=165$ in the parent spectrum. A molecular ion at $m/z=471$ and a fragment at $m/z=181$ suggest a hydroxylated structure with the hydroxyl group on the phenyl-ethyl moiety.

Differently from the profile with cryopreserved hepatocytes, the chromatogram obtained with fresh cells shows an inverted ratio between the two major metabolites whereas the parent compound is almost absent. The absence of hydroxyl derivatives is noteworthy after the incubation with fresh hepatocytes and the increased amount of glucuronides ($\text{RT}=6.64, 6.83$ and 7.00 min with mass $m/z=603$, *O*-nor-verapamil glucuronides; $\text{RT}=6.69, 6.80, 6.88$ and 7.20 min with mass $m/z=617$, *O*-verapamil glucuronides).

In conclusion the profile from cryopreserved hepatocytes is similar to that previously reported [7] whereas the profile deriving from fresh cells is more similar to the findings from in vivo data [7] where phenyl-isopropyl-valeronitrile is the predominant metabolite.

Comparison of the resolution power of UPLC and HPLC was performed on the fresh hepatocytes samples using both the BEH (UPLC mode) and the XBridge column (HPLC mode). See Fig. 7 (inset A for UPLC and inset B for HPLC).

HPLC peaks are broader and less resolved than in the UPLC chromatogram; peaks at 6.9 and 6.99 min in the UPLC chromatogram co-elute at 7.1 min. Spectra of the peak revealed in fact the co-elution of the phenyl-isopropyl-valeronitrile and the

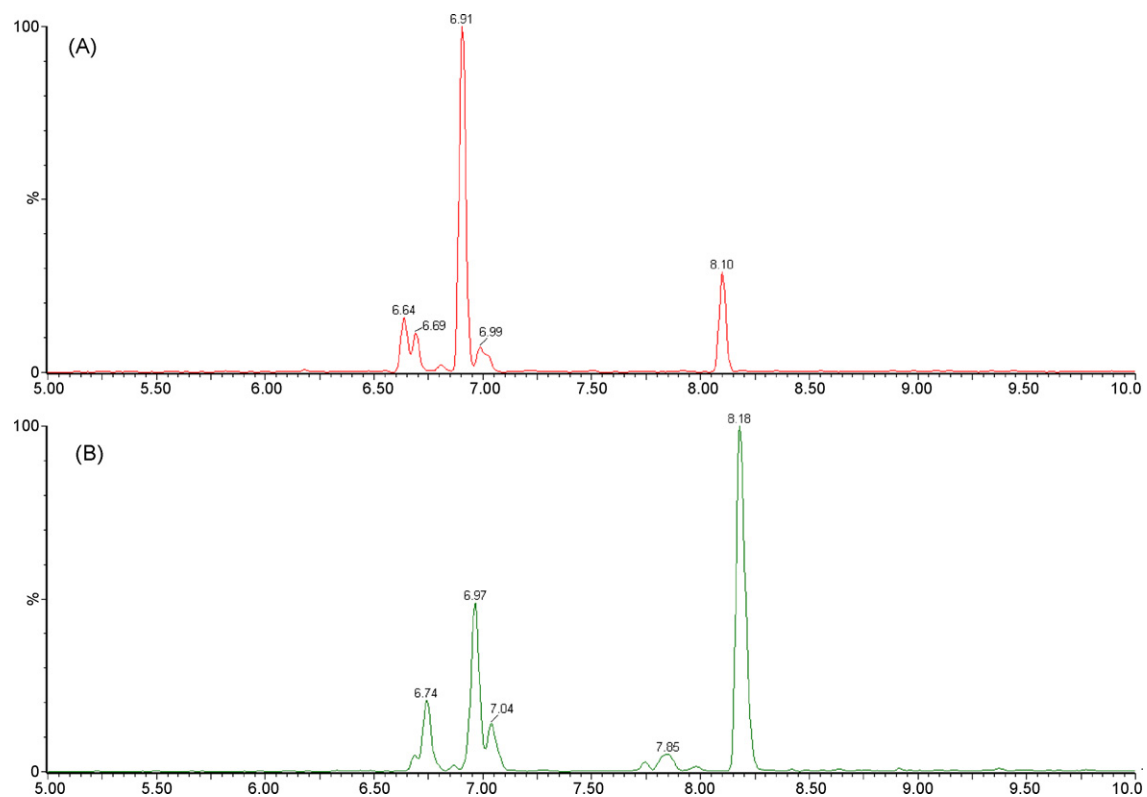


Fig. 6. Reconstructed ion chromatograms from (A) fresh dog hepatocytes and (B) cryopreserved dog hepatocytes. Both the analysis has been acquired on Acquity BEH column. Verapamil peak has been removed for clarity reasons.

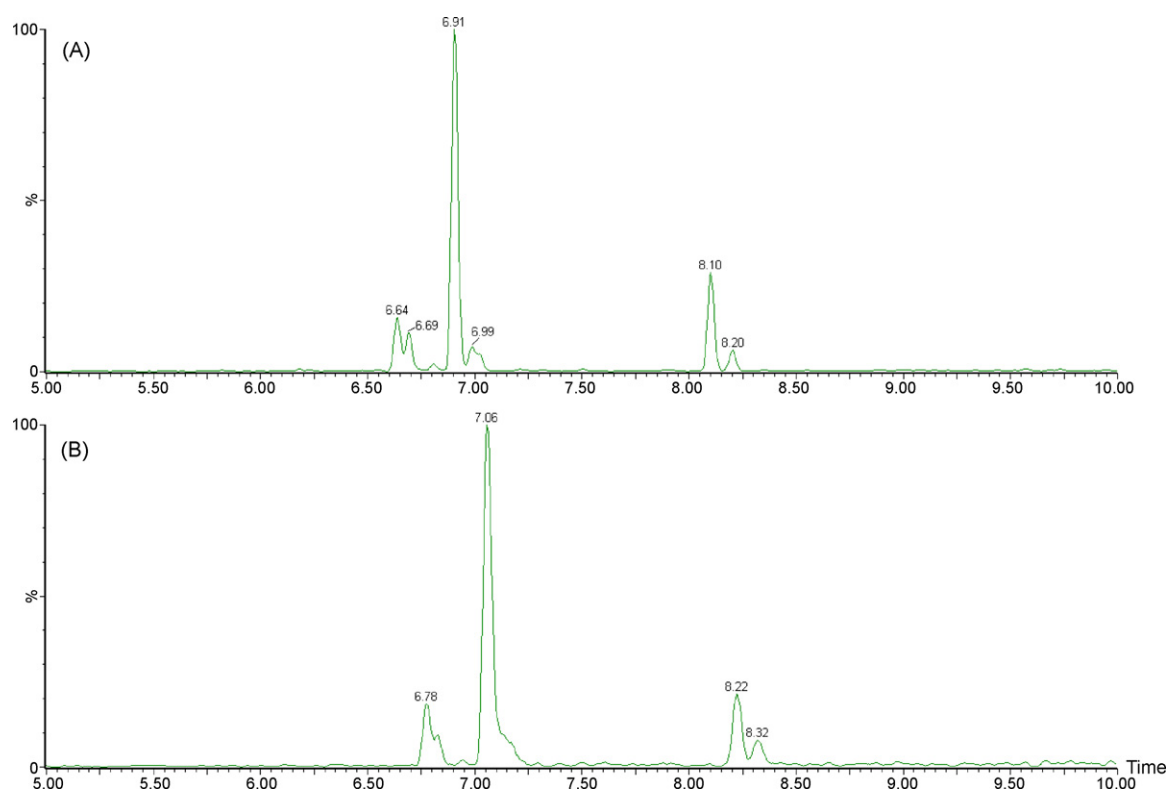
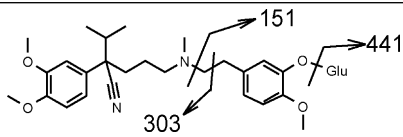
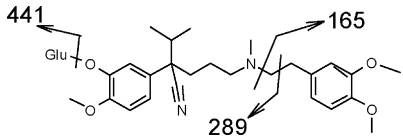
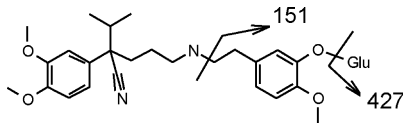
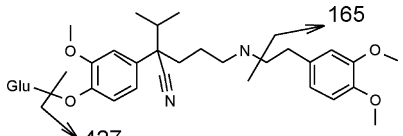
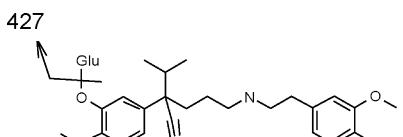
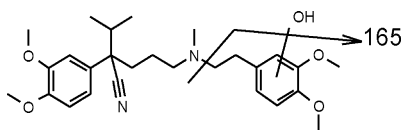
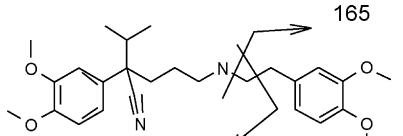
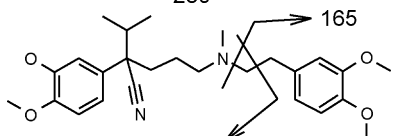
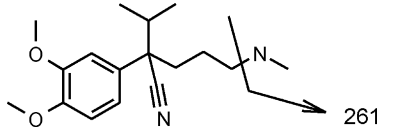


Fig. 7. Reconstructed ion chromatograms obtained from fresh dog hepatocytes incubation analyzed on different columns: (A) Acquity BEH C18 100 mm \times 2.5 mm \times 1.7 μ m and (B) XBridge C18 100 mm \times 2.1 mm \times 3.5 μ m. Verapamil is the last eluted peak in both the chromatograms.

Table 8
Assigned structures and relative fragments of the metabolites

<i>m/z</i> (a.m.u.)	R.T. (min)	Structure	Fresh ^a	Cryo. ^a
617	6.99		5	7
	6.69		6	10
603	7.01		2	n.d.
	6.80		1	2
	6.64		10	2
471	7.95		n.d.	1
441	8.10		17	51
	7.85		n.d.	4
291	6.91		59	24

^aArea% respect to the total of the metabolites.

glucuronides with masses of $m/z = 603$ and $m/z = 617$. Similarly peaks at 6.7 and 6.8 min are less resolved.

4. Conclusions

The new type of liquid chromatography, UPLC, was tested highlighting clear advantages. The most significant is a reduction in the time of analysis resulting also in a reduction in solvent consumption, especially in the analysis of PK or clearance samples coupled with an increase in sensitivity, potentially reducing the impact of the quality of the analyte purification from the biological matrix.

Increased resolution is of clear benefit in the study of metabolites, where greater separation of the peaks allowed the identification of four different glucuronides for each of the major metabolites of verapamil.

Acknowledgement

The authors gratefully acknowledge Dr. Zunino's group from Istituto Nazionale Tumori (Milano, Italy) for animal treatment.

References

- [1] S. Venkatesh, R.A. Lipper, *J. Pharm. Sci.* 89 (2000) 145–154.
- [2] R. Li, L. Dong, J. Huang, *Anal. Chim. Acta* 546 (2005) 167–173.
- [3] L. Nováková, L. Matysová, P. Solich., *Talanta* 68 (3) 908–918.
- [4] J. Borlak, M. Blickwede, T. Hansen, W. Koch, M. Walles, K. Levsen, *Drug Metab. Dispos.* 33 (8) 1108–1114.
- [5] M.K. Bayliss, J.A. Bell, K. Wilson, G.R. Park, *Xenobiotica* 24 (1994) 231–241.
- [6] S.J. Griffin, J.B. Houston, *Drug Metab. Dispos.* 32 (5) 552–558.
- [7] B. Reder-Hilz, M. Ullrich, M. Ringel, N. Hewitt, D. Utesch, F. Oesch, J.G. Hengstler, *Naunyn-Schmiedeberg's Arch. Pharmacol.* 369 (2004) 408–417.